Research Square

Preprints are preliminary reports that have not undergone peer review.
They should not be considered conclusive, used to inform clinical practice,
or referenced by the media as validated information.

Adipocyte-derived FABP4 Drives Pancreatic Cancer Radioresistance via FABP4- eIF3a Axis

Wei MO
Soochow University
Yuji Xiao
Soochow University
Di Chen
Changhai Hospital affiliated to Naval Medical University
Lunjie Lu
Soochow University
Wei Zhu
Soochow University
Jianping Cao
Soochow University
Huojun Zhang
Soochow University
Yang Jiao
jiaoyang@suda.edu.cn
Soochow University

Research Article

Keywords: Pancreatic cancer, radioresistance, adipocytes, fatty acid-binding protein 4 (FABP4), eukaryotic translation initiation factor 3 subunit a (eIF3a)

Posted Date: November 9th, 2026

DOI: https://doi.org/10.21203/rs.3.rs-11643734/v1

License: This work is licensed under a Creative Commons Attribution 4.0 International License.
Read Full License

Additional Declarations: No competing interests reported.

Title: Adipocyte-derived FABP4 Drives Pancreatic Cancer Radioresistance via FABP4-eIF3a Axis

Wei Mo[1, #], Yuji Xiao[1, 2, #], Di Chen[3, #], Lunjie Lu[1, 4], Wei Zhu[1], Jianping Cao[1, *], Huojun Zhang[3, *], Yang Jiao[1, *]

1. State Key Laboratory of Radiation Medicine and Protection, School of Radiation Medicine and Protection, Key Laboratory of Radiation Damage and Treatment of Jiangsu Provincial Universities and Colleges, Collaborative Innovation Center of Radiological Medicine of Jiangsu Higher Education Institutions, Soochow University, Suzhou 215123, China.

2. Department of Radiation Oncology, The Second Affiliated Hospital of Soochow University, Suzhou 215004, China.

3. Department of Radiation Oncology, Changhai Hospital affiliated to Naval Medical University, Shanghai 200433, China.

4. Department of Oncology, Qingdao Central Hospital, University of Health and Rehabilitation Sciences, Qingdao 266042, China.

# These authors contributed equally.

*Corresponding authors: Yang Jiao, jiaoyang@suda.edu.cn; Jianping Cao, jpcao@suda.edu.cn; Huojun Zhang, chyyzhj@163.com

Abstract:

Background: Radiotherapy is a common treatment modality for patients with locally advanced or metastatic pancreatic cancer, but the therapeutic efficacy is constrained by intrinsic radioresistance. The tumor microenvironment, particularly peritumoral adipose tissue, plays a critical yet poorly understood role in modulating

therapeutic responses.

Methods: Peritumoral adipose tissue distribution in pancreatic cancer was assessed by H&E staining. The effects of adipocytes on cancer cell radiosensitivity were evaluated using a co-culture system combined with colony formation, alkaline comet, and flow cytometry assays. Energy metabolism, lipid accumulation, and fatty acid transporter levels in co-cultured cancer cells were examined by Seahorse analysis, BODIPY staining, real-time PCR, and immunofluorescence. The role of FABP4 in adipocyte-mediated radiosensitivity regulation was tested using FABP4-knockout 3T3-L1 cells, exogenous FABP4 protein, and a FABP4 inhibitor. FABP4-overexpressing cancer cells and nude mouse xenografts were used to determine the effects of FABP4 on radiosensitivity. Underlying mechanisms were explored and validated by Co-IP, LC-MS/MS, RIP, and other approaches.

Results: The results of the pathology showed that the pancreatic cancer was surrounded by peripancreatic adipose tissue. Co-culture with adipocytes significantly enhancing clonogenic survival of pancreatic cancer cells while attenuated radiation-induced DNA damage, apoptosis, and G2/M arrest, an effect mediated by FABP4. Genetic ablation of FABP4 in adipocytes abolished this radioprotection, whereas exogenous FABP4 supplementation or its overexpression recapitulated radioresistance both in vitro and in vivo. Proteomic screening identified eIF3a as the predominant FABP4-interacting protein. Functional validation demonstrated that eIF3a knockdown abrogated the FABP4-enhanced radioresistance, confirming its essential role in this process. EIF3a knockdown increased KU80 and MRE11 expression and promoted

radioresistance, whereas FABP4 suppressed KU80 and MRE11 expression by enhancing eIF3a–mRNA binding.

Conclusions: This study identify adipocyte-derived FABP4 as a pivotal regulator of pancreatic cancer radiosensitivity and unveil the FABP4–eIF3a axis as a potential therapeutic target for radiosensitization.

Keywords: Pancreatic cancer, radioresistance, adipocytes, fatty acid-binding protein 4 (FABP4), eukaryotic translation initiation factor 3 subunit a (eIF3a)

Materials and Methods:

Patient specimen collection

Patient tissue sections and peritumoral adipose tissue were obtained from the First Affiliated Hospital of Soochow University (Ethics Committee approval no. 2022336). This study was approved by the Ethics Committee of the First Affiliated Hospital of Soochow University and was conducted in accordance with the Declaration of Helsinki. Written informed consent was obtained from each patient.

Hematoxylin and eosin (H&E) staining

The Pancreatic tissues were fixed in 10% neutral-buffered formalin and embedded in paraffin. Three-micrometer paraffin sections were deparaffinized and heat-treated using citrate buffer (pH 6.0) for 7 min following an epitope retrieval protocol. The sections were stained using H&E (ZSGB-Bio, Beijing, China).

Cell culture and irradiation treatment

Adipocytes from adipose tissues were isolated as previously described methodologies

[1]. Adipose deposits were digested for one hour at 37 °C using Dulbecco's Modified Eagle's Medium (DMEM) containing collagenase type I (1 mg/mL) and 0.1 % BSA. Mature adipocytes were collected from the upper phase following centrifugation at 100×g for 3 minutes. Human pancreatic cancer cell lines PANC-1 and SW1990, human embryonic kidney 293T cells, and mouse 3T3-L1 preadipocytes were maintained at 37 °C in a humidified incubator containing 5% CO_2. PANC-1 and SW1990 cells were cultured in RPMI-1640 medium; 293T and 3T3-L1 cells in DMEM, all supplemented with 10% FBS. For co-cultures, the transwell culture system (0.4-μm pore size, Corning, NY, USA) was used. A total of 1×10^5 adipocytes were placed in the upper chamber, while 1×10^5 PANC-1 or SW1990 cells were seeded in the bottom. PANC-1 or SW1990 cells were grown in monocultures (in the absence of adipocytes) in the culture medium. The cells were irradiated using an X-ray linear accelerator (Rad Source, GA, USA) at a fixed dose rate of 1.15 Gy/min.

Colonogenic Assay

Cells were counted and plated in 6-well plates at 2×10^2, 4×10^2, 8×10^2, 1.6×10^3, or 3.2×10^3 cells/well, then irradiated 24 h later with 0, 2, 4, 6, or 8 Gy. After 2 weeks, visible colonies were fixed with 4% paraformaldehyde (30 min), stained with crystal violet (30 min, RT; Beyotime), and colonies containing ≥50 cells were counted. Plating efficiency (PE) = (colonies/inoculated cells) × 100%; Survival fraction (SF) was calculated from treated colonies and corrected by PE.

Immunofluorescence microscopy

The cells were seeded onto glass coverslips in 24-well plates and cultured overnight.

At various time points after 6 Gy irradiation, cells were fixed with 4% paraformaldehyde for 30 min at room temperature, permeabilized with 0.5% Triton X-100 for 10 min on ice, and blocked with 5% BSA for 60 min. The cells were then incubated with primary antibodies, followed by incubation with secondary antibodies. The slides were washed and counterstained with DAPI. Images were acquired using confocal microscopy (Olympus, Tokyo, Japan).

Flow cytometry assay

Flow cytometry was used to evaluate apoptosis and cell cycle distribution in PANC-1 and SW1990 cells. For apoptosis analysis, cells were harvested 72 h after 6 Gy X-ray irradiation, trypsinized, washed, and resuspended in annexin-binding buffer. After staining with Annexin V-FITC and PI (BD Biosciences, NJ, USA) for 20 min in the dark, samples were analyzed on a BD FACS Calibur flow cytometer (BD Biosciences, NJ, USA). For cell cycle analysis, cells were seeded in six-well plates and transiently transfected, followed by 6 Gy X-ray irradiation and culture for 24 h. Cells were then fixed in 70% ethanol at 4°C overnight and stained using the Cell Cycle and Apoptosis Analysis Kit (Beyotime, Nanjing, China) according to the manufacturer's instructions; cell cycle distribution was determined by flow cytometry.

Animal study

BALB/c nude mice (male, 16-18 g and 5 weeks old) were purchased from Shanghai SLAC laboratory Animal Co., Ltd. All animal experiments were approved by the Ethics Committee of Soochow University (Approval No. SUDA20221024A02) and were conducted in accordance with the Guide for the Care and Use of Laboratory Animals.

All male BALB/c nude mice were randomly assigned to 4 groups (n = 4 per group): ad-NC, ad-FABP4, IR + ad-NC or IR + ad-FABP4. The subcutaneous xenograft model was established. Tumor size was measured every other day, and the tumor volume was calculated with the equation V (in mm^3) = 1/2× L× W^2 (L: length; W: width). A 160 KeV X-ray linear accelerator (Rad Source Technologies, GA, USA) with a dose rate of 1.214 Gy/min (10 Gy) was used for animal irradiation.

Immunohistochemistry (IHC) staining

IHC staining was performed using the Vectastain ABC kit (Vector Laboratories, Newark, CA) according to the manufacturer's instructions. Sections of paraffin-embedded xenograft tumors were stained with antibodies against FABP4, Ki67, and caspase-3. Nonspecific IgG was used as a negative control. The staining of the tissues was quantitatively scored according to the percentage of positive cells and the staining intensity.

Reagents

Antibodies: Anti-FABP4 (Abcam, ab92501), Anti-γH2AX (Abcam, ab81299), Anti-eIF3a (CST, 2538), Anti-Mre11 (CST, 4895), Anti-Ku80 (CST, 2753), Anti-Rad50 (CST, 3427), and anti-GAPDH (Beyotime, AB0037) antibodies were used. Secondary antibodies, Cy3-labeled Goat Anti-Rabbit IgG (H+L) antibody (Beyotime, A0516) and FITC-labeled Goat Anti-Rabbit IgG (H+L) antibody (Beyotime, A0562), were employed. Adenovirus vectors encoding Flag-tagged FABP4 and corresponding control vectors were generated by WeiZhen Biosciences (Shandong, China). Human eIF3a siRNA (HSS112707) and Silencer Negative Control siRNA were purchased from

Invitrogen (MA, USA).

Cell BODIPY staining analysis

For BODIPY staining, cells were treated with 4% paraformaldehyde (Sigma-Aldrich, MO, USA) for 15 min and then treated with BODIPY reagent (Beyotime, Nanjing, China) for 20 min. All images were captured using confocal microscopy (Olympus, Tokyo, Japan)

Co-immunoprecipitation (Co-IP)

A Co-immunoprecipitation assay was performed using the Pierce Co-Immunoprecipitation Kit (Thermo Scientific, 26149) in accordance with the manufacturer's instructions. In brief, antibodies were immobilized on AminoLink Plus Coupling Resin by rotating at room temperature for two hours. Cells were lysed on ice using ice-cold IP Lysis/Wash Buffer and then centrifuged at 13,000 g for ten minutes. The supernatants were then incubated with the bait-prey protein mixture at 4°C overnight, followed by elution steps. A 5× Lanes Marker Sample Buffer was added to the samples buffer, and the samples were heated at 95–100°C for 5 min before being applied to the gel.

liquid chromatography-tandem mass spectrometry (LC-MS/MS)

Protein samples were separated into two fractions by SDS-PAGE. The corresponding gel bands were excised and subjected to in-gel digestion to generate peptides. The resulting peptides were separated by online liquid chromatography and analyzed using a SCIEX TripleTOF 5600 mass spectrometer (AB SCIEX, CA, USA). Each fraction was analyzed twice by mass spectrometry. Protein identification was performed using

ProteinPilot software (version 4.5; AB SCIEX, CA, USA) against the human Swiss-Prot protein database.

RNA-binding protein immunoprecipitation (RIP)

The RIP assay was conducted in accordance with the instructions provided in the EZ-Magna RNA Immunoprecipitation (RIP) Kit (Millipore). For this experiment, 293T cells were harvested and lysed in ice-cold lysis buffer containing RNase and protease inhibitor for 20 minutes. Subsequently, the cell lysates were centrifuged, and the supernatant was incubated with anti-rabbit IgG or anti-rabbit eIF3a antibodies with rotation at 4°C overnight. Subsequently, the immunoprecipitated RNA was isolated and the expression of Rad50, Ku80, and Mre11 mRNA was quantified using a reverse transcription polymerase chain reaction (RT-PCR) assay.

Statistical analysis

All experiments involving cell lines were conducted in triplicate. The results are presented as the mean ± standard error of the mean (SEM). The data were subjected to statistical analysis using GraphPad Prism (version 10.1.2). A two-tailed Student's t-test was employed for the comparison of two groups prior to journal submission, while a one-way ANOVA with Tukey post hoc analysis was utilized for the comparison of multiple groups. *$p < 0.05$, **$p < 0.01$, ***$p < 0.001$ were considered statistically significant.

Introduction

Pancreatic cancer (PC) is among the most lethal malignancies worldwide, with a

5-year survival rate of approximately 13% [2]. Although radiotherapy techniques, including stereotactic body radiotherapy (SBRT) and proton therapy, have advanced, the clinical benefit of radiotherapy for PC patients remains limited by the inherent and acquired radioresistance of pancreatic cancer cells [3, 4].

The tumor microenvironment (TME) has emerged as a critical determinant of therapeutic response [5]. Among its stromal components, peritumoral adipose tissue is increasingly recognized as an active participant in cancer progression. The incidence of PC is closely associated with obesity, and PC cells are frequently surrounded by abundant peripancreatic fat. Adipocytes constitute a prominent component of this adipose-enriched TME. Peritumoral adipocytes promote cancer progression through the secretion of adipokines, free fatty acids, and cytokines [6–11]. However, whether adipocytes influence the response of PC cells to ionizing radiation (IR) remains largely unexplored.

Fatty acid-binding proteins (FABPs) are cytoplasmic lipid chaperones that regulate intracellular fatty acid trafficking and metabolic homeostasis [12]. Tumor microenvironmental signals, including adipocyte-derived lipids and obesity-associated fatty acids, can regulate FABP expression [13]. Increasing evidence identifies FABPs as key drivers of tumor metabolic reprogramming. FABP4, a member of the FABP family, plays crucial roles not only in cell signaling and metabolic regulation but also in the pathogenesis of metabolic disorders, inflammation, and cancer [14, 15]. Elevated FABP4 expression in PC tissues is associated with lymph node metastasis, advanced disease stage, and poor prognosis [16]. Consistent with this, FABP4 inhibition

suppresses PC progression and metastasis [17]. Furthermore, our previous study demonstrated that adipocytes promote cholangiocarcinoma metastasis via FABP4 [18]. Moreover, FABP4 has been shown to mediate chemoresistance in ovarian and breast cancers, suggesting a broader role for FABP4 in therapy resistance [16, 17, 19–21]. In addition, adipocyte-derived FABP4 can attenuate radiation-induced oxidative damage in dermal tissue [1, 22]. Although these studies implicate FABP4 in adipocyte-induced radioresistance in PC, direct evidence is still lacking.

In this study, the role of adipocyte-derived FABP4 in pancreatic cancer radioresistance was investigated using co-culture models, genetic loss-of-function approaches, proteomic screening, and in vivo xenograft assays. We identified a novel FABP4–eIF3a signaling axis that promotes radioresistance by mediating adipocyte–cancer cell crosstalk that mitigates radiation-induced damage. Collectively, these findings establish the FABP4–eIF3a pathway as a promising therapeutic target for radiosensitization in PC. Further elucidation of the role of FABP4 in regulating PC radiosensitivity and of the underlying molecular mechanisms may reveal additional radiosensitization targets.

Results:

Adipocytes promote radioresistance of pancreatic cancer cells

The pancreas, surrounded by adipose tissue, interacts with neighbouring adipose tissue as cancer progresses (Fig. 1A). We studied how adipocytes affect cancer cell radiosensitivity. Using clonogenic assays, the gold standard in radiobiology, we showed

that culturing cancer cells with adipocytes reduced the radiosensitivity of a particular type of cancer cell (Fig. 1B). This was marked by a higher D0 value in the co-cultured group than that in the control one (2.297 vs 1.041). The SER of the co-cultured cells was 0.453, indicative of higher radioresistance. To detect DNA damage, an alkaline comet assay was used; at 1 h after irradiation, less DNA damage was seen in the co-cultured cells (Fig. 1C&D). An immunofluorescence assay was then used to visualize the γ-H2AX foci. As shown in Fig. 1E and F, a significant decrease in the number of γ-H2AX foci per nucleus was determined in the co-cultured cells, indicating reduced nuclear DNA damage in pancreatic cancer cells after irradiation.

Subsequently, cell cycle distribution and apoptosis were analyzed using flow cytometry after X-ray exposure (Fig. 1G–J). As shown in Fig. 1G and H, irradiation-induced G2/M phase arrest was more pronounced in the control group than in the co-culture group. Additionally, adipocyte co-culture did not affect basal apoptosis but reduced radiation-induced apoptosis in both cell lines (from 18.91% to 11.65% in PANC-1 cells; from 17.22% to 12.23% in SW1990 cells) (Fig. 1I&J). Collectively, these findings suggest that adipocyte co-culture promotes radioresistance in pancreatic cancer cells, potentially by reducing nuclear DNA damage, suppressing apoptosis, and alleviating G2/M phase arrest.

FABP4 mediates the adipocyte-triggered radioresistance of pancreatic cancer cells.

Adipocytes supply tumour cells with fatty acids, thereby affecting their energy metabolism and promoting tumour growth [23]. In this study, co-culture with adipocytes caused lipid droplet accumulation in the PANC-1 cells (Fig. 2A) and

elevated glycolytic activity after irradiation (Fig. S1). Free fatty acids from adipose tissue require FABPs for transport. Real-time PCR analysis revealed that FABP4 was the only FABP that increased in the pancreatic cancer cells following co-culture (Fig. 2B&D).

Stable FABP4-knockout 3T3-L1 cells were established to investigate the role of FABP4 in radiosensitivity and the effects of adipocytes on radiation-induced apoptosis and G2/M arrest in pancreatic cancer cells (Fig. S2). The protective effect of the 3T3-L1 cells was reduced when FABP4 was deleted (Fig. 2E–H), and addition of the FABP4 inhibitor BMS309403 reversed alterations in γ-H2AX foci formation, mitochondrial membrane potential and cell cycle progression in the pancreatic cancer cells (Fig. 2I–K). Furthermore, exogenous FABP4 (eFABP4) altered radiosensitivity (Fig. S3) and modulated endogenous FABP4 expression in PANC-1 cells (Fig. S4). In conclusion, adipocyte-derived FABP4 increases radioresistance in pancreatic cancer cells by reducing DNA damage, suppressing cell death and alleviating G2/M arrest.

FABP4 regulates the radiosensitivity of pancreatic cancer both in vitro and in vivo

To examine the role of FABP4 in PC radiosensitivity, FABP4-overexpressing cells were used (Fig. S4C). Cells overexpressing FABP4 showed significant radioresistance in clonogenic assays (Fig. 3A). For example, the surviving fractions after 4 Gy irradiation (SF4) were 24.6% and 42.95% for the control and FABP4-overexpressing PANC-1 cells, with an SER of 0.775. The comet assay revealed significantly reduced DNA damage in FABP4-overexpressing pancreatic cells (Fig. 3B). Immunofluorescence showed FABP4 overexpression decreased radiation-induced γ-

H2AX foci formation (Fig. 3C&D). Flow cytometry confirmed reduced apoptosis and G2/M arrest (Fig. 3E–H). Moreover, FABP4 overexpression reversed radiation-induced changes in mitochondrial membrane potential (Fig. 3I).

In nude mice, irradiation reduced subcutaneous tumor size, but tumors overexpressing FABP4 had larger volumes after irradiation (Fig. 3J). This indicates that FABP4 overexpression promotes radioresistance *in vivo*. Irradiation downregulated Ki67 and upregulated cleaved caspase-3 in the tumors, and these changes were reversed by FABP4 overexpression (Fig. 3K). Collectively, these results indicate that FABP4 promotes radioresistance both in vitro and in vivo.

eIF3a mediates FABP4-induced radioresistance in pancreatic cancer cells

To elucidate the mechanism by which FABP4 enhances radioresistance in cancer cells, liquid chromatography-tandem mass spectrometry (LC-MS/MS) was performed. This proteomic screen initially identified 142 proteins that potentially interact with FABP4 and may be involved in regulating radiosensitivity (Fig. S5A). Among these candidates, eIF3a was identified as the top-ranked interacting partner (Fig. 4A&B, Table 1). The physical interaction between FABP4 and eIF3a was subsequently validated in PANC-1 cells via co-immunoprecipitation (Co-IP). As shown in Fig. 4C, FABP4 co-immunoprecipitated with endogenous eIF3a.

To determine whether eIF3a mediates the radioprotective effect conferred by FABP4 overexpression, eIF3a was knocked down in FABP4-overexpressing pancreatic cancer cells (Fig. S5B). Alkaline comet assay revealed that eIF3a knockdown abolished the protective effect of FABP4 overexpression against radiation-induced DNA damage,

with comet tail lengths comparable to those in controls (Fig. 4D). Immunofluorescence staining demonstrated that eIF3a knockdown eliminated the FABP4-mediated reduction in γ-H2AX foci formation, with no significant difference from the controls (Fig. 4E&F). Furthermore, flow cytometric analysis showed that eIF3a knockdown reversed the suppressive effects of FABP4 on radiation-induced G2/M arrest and apoptosis, restoring both parameters to control levels (Fig. 4G&H). Collectively, these findings identify eIF3a as a key mediator of FABP4-induced radioresistance in pancreatic cancer cells.

eIF3a mediates FABP4-induced radioresistance in pancreatic cancer cells independently of NHEJ signaling

To elucidate the mechanism by which eIF3a mediates FABP4-induced radioresistance, eIF3a was knocked down using eIF3a siRNA. Knockdown efficiency was confirmed at the protein and mRNA levels (Fig. S6A&B). Clonogenic survival assays showed that IR significantly inhibited the colony-forming ability of control cells, whereas eIF3a-silenced cells exhibited greater radiation resistance (Fig. 5A). Furthermore, eIF3a downregulation reduced irradiation-induced γ-H2AX foci formation in PANC-1 cells (Fig. 5B&C). It was also shown that eIF3a knockdown reduced radiation-induced apoptosis in pancreatic cancer cells (Fig. 5D&E).

EIF3a has been shown to regulate cellular sensitivity to DNA-damaging agents by controlling the synthesis of DNA repair proteins [24]. In the present study, knockdown of eIF3a increased KU80 and MRE11 protein levels, consistent with previous reports (Fig. 5F). RNA-binding protein immunoprecipitation (RIP) was then performed, and

the results showed that FABP4 enhanced the binding of eIF3a to the mRNAs encoding the DNA repair proteins KU80 and MRE11 following IR (Fig 5F). In addition, FABP4 overexpression was found to reduce KU80 and MRE11 protein levels (Fig. 5G). These findings suggest that eIF3a knockdown promotes radioresistance, while FABP4 suppresses KU80 and MRE11 expression by enhancing eIF3a–mRNA binding.

Discussion:

Pancreatic cancer develops in a lipid-rich niche where adipocytes are a major stromal component. Adipocytes have emerged as critical mediators of the obesity–cancer axis in the tumor microenvironment, particularly in malignancies arising in or near adipose depots. As the principal cellular components of adipose tissue, adipocytes play a pivotal role in metabolic homeostasis and, concurrently, in the promotion of disease progression by releasing lipids, mitogens, and pro-inflammatory cytokines [25]. In this study, an adipocyte–pancreatic cancer cell co-culture model was used. Co-culture with adipocytes significantly reduced radiation-induced DNA single-strand breaks and γ-H2AX foci formation, as well as G2/M arrest and apoptosis, while enhancing clonogenic survival. These findings are consistent with recent studies showing that the tumor microenvironment (TME), particularly adipose tissue, actively participates in modulating therapeutic responses in cancer [18, 26, 27]. Given that the pancreas is surrounded by abundant adipose depots and that pancreatic cancer cells frequently infiltrate these depots, these results carry important clinical implications.

The interaction between adipocytes and cancer cells mainly involves adipokines

and fatty acids. In several cancer types, adipocyte-derived fatty acids protect cancer cells from apoptosis and promote treatment resistance by serving as metabolic fuels [23]. Co-culture with adipocytes has been shown to increase the number of lipid droplets in breast cancer cells [28]. In the present study, co-culture with adipocytes induced lipid droplet accumulation and increased glycolytic activity in PANC-1 cells. FABPs are intracellular carriers that bind and transport long-chain fatty acids. They participate in the interaction between adipocytes and cancer cells. Therefore, FABPs represent promising targets for reducing adipose tissue-mediated cancer promotion. A study proposed that fatty acids might activate PPARγ to induce the expression of fatty acid transporters (e.g., FABP4) and anti-apoptotic proteins [29]. In this study, real-time PCR analysis and immunofluorescence staining identified FABP4 as the only FABP upregulated following co-culture. These findings suggest that FABP4 may serve as a key mediator of adipocyte-induced metabolic reprogramming in pancreatic cancer cells, which warrants further investigation into its functional role in radioresistance.

Consistent with this notion, FABP4 was identified as a critical regulator of lipid responses in ovarian cancer cells co-cultured with adipocytes [30]. A previous study demonstrated that adipocytes promote cholangiocarcinoma metastasis through FABP4 [18]. Although FABP4 has been suggested to play a role in adipocyte-regulated tumor progression and in radiation injury to skin tissue, the functional and mechanistic roles of adipocyte-derived FABP4 in tumor radiosensitivity remain unknown. In this study, co-culture with FABP4-knockout 3T3-L1 adipocytes completely abrogated the radioprotective effect, whereas treatment with recombinant FABP4 protein or

overexpression of endogenous FABP4 recapitulated the radioresistant phenotype both in vitro and in vivo. Notably, exogenous FABP4 was demonstrated to be internalized by pancreatic cancer cells and to upregulate endogenous FABP4 expression, suggesting a positive feedback loop that may amplify the radioprotective effect. The in vivo finding that FABP4-overexpressing tumors were larger than controls after irradiation underscores the clinical relevance of this pathway. These data provide further evidence that FABP4 plays a critical role in adipocyte-mediated regulation of radiation resistance in pancreatic cancer cells.

To dissect the downstream mechanisms, LC-MS/MS was performed. This approach identified eIF3a as the predominant FABP4-interacting protein. We further validated this interaction by showing that eIF3a knockdown in FABP4-overexpressing cells abrogated FABP4-enhanced radioresistance, highlighting the critical role of eIF3a in FABP4-mediated regulation of pancreatic cancer radiosensitivity.

As the largest subunit of the eIF3 complex, eIF3a plays a key role in translation and has been implicated in tumorigenesis, cell differentiation, DNA synthesis and repair, and fibrosis [31–35]. eIF3a has previously been implicated in modulating DNA repair and chemosensitivity, primarily through regulation of the non-homologous end joining (NHEJ) pathway, the principal mechanism for repairing radiation-induced DSBs [36]. In the present study, eIF3a knockdown alone, in the absence of FABP4 overexpression, increased radioresistance, as evidenced by enhanced clonogenic survival, reduced γ-H2AX foci, and decreased apoptosis. Consistent with its established role in suppressing NHEJ repair [24], eIF3a knockdown increased KU80 and MRE11 protein levels.

Notably, FABP4 overexpression enhanced the binding of eIF3a to mRNAs encoding the NHEJ repair proteins KU80 and MRE11 while reducing reduced KU80 and MRE11 protein levels, whereas eIF3a knockdown increased them. Nevertheless, both manipulations converged on enhanced radioresistance. Specifically, whereas eIF3a knockdown relieves suppression of canonical NHEJ, increasing repair proteins and conferring modest resistance, FABP4 binding redirects eIF3a toward a distinct program that independently promotes survival. This apparent paradox suggests that the FABP4–eIF3a axis regulates radiosensitivity independently of canonical NHEJ; the mechanisms underlying this regulation warrant further investigation.

In conclusion, this study establishes that adipocyte-derived FABP4 drives radioresistance in pancreatic cancer through a previously unrecognized FABP4–eIF3a regulatory axis. These findings not only advance our understanding of tumor–adipose crosstalk but also identify FABP4 and eIF3a as promising therapeutic targets for overcoming radiation resistance in this refractory malignancy.

While these findings hold significant promise, several limitations remain in the current study. First, it remains unknown precisely how FABP4 enhances eIF3a binding to KU80 and MRE11 mRNAs and how this interaction alters eIF3a's function. It is possible that FABP4 directly binds eIF3a and induces a conformational change that relieves autoinhibition or alters mRNA selectivity. Alternatively, FABP4 may serve as a bridging factor between eIF3a and specific RNA sequences. Second, while we focused on KU80 and MRE11, we cannot exclude the possibility that other NHEJ repair proteins, or even alternative DNA repair pathways, are also regulated by the

FABP4-eIF3a axis. Moreover, the present data do not establish whether eIF3a mediates radioresistance through KU80/MRE11 or through a broader eIF3a-dependent translational program. Further experiments are required to answer these questions. Finally, because all evidence is derived from cultured pancreatic cancer cells and subcutaneous xenografts, the clinical relevance of FABP4–eIF3a-axis activity as a determinant of radioresponse remains untested in patient-derived tissue or radiotherapy cohorts.

Abbreviations

LC-MS/MS	liquid chromatography-tandem mass spectrometry
Co-IP	Co-immunoprecipitation
DSBs	Double-strand breaks
EIF3a	Eukaryotic translation initiation factor 3 subunit a
FABP4	Fatty acid-binding protein 4
FABPs	Fatty acid-binding proteins
H&E	Hematoxylin and eosin
IR	Ionizing radiation
NHEJ	Non-homologous end joining
PC	Pancreatic cancer
qRT-PCR	Quantitative reverse transcription polymerase chain reaction
RIP	RNA immunoprecipitation
SBRT	Stereotactic body radiotherapy
SDS–PAGE	Sodium dodecyl sulfate–polyacrylamide gel electrophoresis
SER	Sensitization enhancement ratio
SF4	Surviving fractions after 4 Gy irradiation
SF	Survival fraction

SSBs	Single-strand breaks
TME	Tumor microenvironment

Declarations

Ethics approval and consent to participate: The human sample study was approved by and the Ethics Committee of the First Affiliated Hospital of Soochow University and fulfilled the Declaration of Helsinki Principles (Ethics Committee No. 2022336). All animal experiments were approved by the Ethics Committee of Soochow University (Approval No. SUDA20221024A02) and were conducted in accordance with the Guide for the Care and Use of Laboratory Animals.

Consent for publication: Not applicable.

Availability of data and materials: The datasets used and/or analyzed during the current study are available from the corresponding author on reasonable request.

Competing interests: The authors declare that they have no competing interests.

Funding

This work was supported by the National Natural Science Foundation of China (grant numbers: 82473233, 82303680, 82304070, 81773226), the National key R&D Program of China (2022YFC2503700, 2022YFC2503703), Suzhou Fundamental Research Project (SJC2023001), A Project Funded by the Priority Academic Program Development of Jiangsu Higher Education Institutions (PAPD), Postgraduate Research & Practice Innovation Program of Jiangsu Province (KYCX24_3334).

Authors' contributions: Yang Jiao, Huojun Zhang and Jianping Cao designed the research and supervised the study. Wei Mo, Yuji Xiao, Di Chen and Lunjie Lu

performed the experiments, Wei Zhu and Di Chen analyzed the data. Wei Mo wrote the manuscript and Yang Jiao supervised the revision of the manuscript.

Acknowledgements: We sincerely thank all the patients for their invaluable participation in this study.

Additional file 1:

File format: .docx

Title: Supplementary methods, figures and tables

Description: This file contains supplementary methods, six supplementary figures (Figures S1–S6) and one supplementary table (Table S1). The supplementary methods include the alkaline comet assay, Seahorse analysis, siRNA transfection, real-time PCR and Western blot.

Figure S1. Adipocyte co-culture increased glycolysis in PANC-1 cells.

Figure S2. Establishment of stable FABP4-knockout 3T3-L1 cells.

Figure S3. eFABP4 enhances the radioresistance of pancreatic cancer cells.

Figure S4. Effects of recombinant human FABP4 protein (eFABP4) on endogenous FABP4 expression.

Figure S5. Identification of FABP4-interacting proteins by LC-MS/MS and validation of eIF3A knockdown.

Figure S6. Knockdown efficiency of eIF3A at the mRNA and protein levels in PANC-1 cells.

Table S1. Primer sequences.

References

1. Xiao Y, Mo W, Jia H et al. Ionizing radiation induces cutaneous lipid remolding and skin adipocytes confer protection against radiation-induced skin injury. J Dermatol Sci. 2020; 97(2):152-60. https://doi.org/10.1016/j.jdermsci.2020.01.009
2. Siegel RL, Kratzer TB, Wagle NS et al. Cancer statistics, 2026. CA Cancer J Clin. 2026; 76(1):e70043. https://doi.org/10.3322/caac.70043
3. Dardare J, Martz N, Witz A et al. Improving Radiation Therapy in Pancreatic Cancer Through Radiosensitization Strategies. Int J Radiat Oncol Biol Phys. 2026; 124(2):395-414. https://doi.org/10.1016/j.ijrobp.2025.09.013
4. Waissi W, Paix A, Nicol A et al. Targeting DNA repair in combination with radiotherapy in pancreatic cancer: A systematic review of preclinical studies. Crit Rev Oncol Hematol. 2020; 153:103060. https://doi.org/10.1016/j.critrevonc.2020.103060
5. Argentiero A, Andriano A, Caradonna IC et al. Decoding the Intricate Landscape of Pancreatic Cancer: Insights into Tumor Biology, Microenvironment, and Therapeutic Interventions. Cancers (Basel). 2024; 16(13). https://doi.org/10.3390/cancers16132438
6. Incio J, Liu H, Suboj P et al. Obesity-Induced Inflammation and Desmoplasia Promote Pancreatic Cancer Progression and Resistance to Chemotherapy. Cancer Discov. 2016; 6(8):852-69. https://doi.org/10.1158/2159-8290.CD-15-1177
7. Arkan MC. Cancer: Fat and the fate of pancreatic tumours. Nature. 2016; 536(7615):157-8. https://doi.org/10.1038/nature19419
8. La Camera G, Gelsomino L, Malivindi R et al. Adipocyte-derived extracellular vesicles promote breast cancer cell malignancy through HIF-1alpha activity. Cancer Lett. 2021; 521:155-68. https://doi.org/10.1016/j.canlet.2021.08.021
9. Bouche C, Quail DF. Fueling the Tumor Microenvironment with Cancer-Associated Adipocytes. Cancer Res. 2023; 83(8):1170-2. https://doi.org/10.1158/0008-5472.CAN-23-0505
10. Huang R, Wang Z, Hong J et al. Targeting cancer-associated adipocyte-derived CXCL8 inhibits triple-negative breast cancer progression and enhances the efficacy of anti-PD-1 immunotherapy. Cell Death Dis. 2023; 14(10):703. https://doi.org/10.1038/s41419-023-06230-z
11. Attane C, Muller C. Drilling for Oil: Tumor-Surrounding Adipocytes Fueling Cancer. Trends Cancer. 2020; 6(7):593-604. https://doi.org/10.1016/j.trecan.2020.03.001
12. Wu L, Ou GL, Zhang W et al. Fatty acid-binding proteins in cancers. Int J Surg. 2025; 111(11):8402-22. https://doi.org/10.1097/JS9.0000000000003049
13. Sun F, Zhang H, Cao H et al. FABPs-mediated lipid signaling pathways in tumor reprogramming: bidirectional crosstalk with the immune microenvironment. Bioorg Chem. 2026; 182:110484. https://doi.org/10.1016/j.bioorg.2026.110484
14. Wang M, Hawanga M, Wan S et al. FABP4 in lipid metabolism and the tumor microenvironment: mechanisms and therapeutic potential. Lipids Health Dis. 2025; 25(1):29. https://doi.org/10.1186/s12944-025-02833-x
15. Majchrzak K, Piotrowska M, Krajewska J et al. Adipocyte Fatty Acid Binding Protein (A-

FABP) as a Potential New Therapeutic Target for the Treatment of Obesity - Associated Cancers. Curr Drug Targets. 2022; 23(6):597-605. https://doi.org/10.2174/1389450122666210712193654
16. Luo Y, Liu S, Yao K. Transcriptome-wide Investigation of mRNA/circRNA in miR-184 and Its r.57c > u Mutant Type Treatment of Human Lens Epithelial Cells. Molecular therapy Nucleic acids. 2017; 7:71-80. https://doi.org/10.1016/j.omtn.2017.02.008
17. Shinoda S, Nakamura N, Inoko K et al. Inhibition of fatty acid binding protein suppresses pancreatic cancer progression and metastasis. Sci Rep. 2025; 15(1):26084. https://doi.org/10.1038/s41598-025-11271-9
18. Nie J, Zhang J, Wang L et al. Adipocytes promote cholangiocarcinoma metastasis through fatty acid binding protein 4. Journal of experimental & clinical cancer research : CR. 2017; 36(1):183. https://doi.org/10.1186/s13046-017-0641-y
19. Sun N, Zhao X. Therapeutic Implications of FABP4 in Cancer: An Emerging Target to Tackle Cancer. Front Pharmacol. 2022; 13:948610. https://doi.org/10.3389/fphar.2022.948610
20. Yang J, Liu S, Li Y et al. FABP4 in macrophages facilitates obesity-associated pancreatic cancer progression via the NLRP3/IL-1beta axis. Cancer Lett. 2023; 575:216403. https://doi.org/10.1016/j.canlet.2023.216403
21. Smolinska K, Szopa A, Dobrowolski P et al. Targeting fatty acid-binding protein 4: A therapeutic intersection of obesity and cancer via lipid metabolism. Prog Lipid Res. 2025; 100:101353. https://doi.org/10.1016/j.plipres.2025.101353
22. Sun C, Song B, Sheng W et al. Fenofibrate Attenuates Radiation-Induced Oxidative Damage to the Skin through Fatty Acid Binding Protein 4 (FABP4). Front Biosci (Landmark Ed). 2022; 27(7):214. https://doi.org/10.31083/j.fbl2707214
23. Dumas JF, Brisson L. Interaction between adipose tissue and cancer cells: role for cancer progression. Cancer Metastasis Rev. 2021; 40(1):31-46. https://doi.org/10.1007/s10555-020-09934-2
24. Tumia R, Wang CJ, Dong T et al. eIF3a Regulation of NHEJ Repair Protein Synthesis and Cellular Response to Ionizing Radiation. Front Cell Dev Biol. 2020; 8:753. https://doi.org/10.3389/fcell.2020.00753
25. Calabrese C, Miserocchi G, De Vita A et al. Lipids and adipocytes involvement in tumor progression with a focus on obesity and diet. Obes Rev. 2024; 25(12):e13833. https://doi.org/10.1111/obr.13833
26. Wang JH, Zheng YQ, Qian ZY et al. Peritumoural adipose tissue drives immune evasion in colorectal cancer via adipose-mesenchymal transformation. Nat Cell Biol. 2026; 28(3):581-95. https://doi.org/10.1038/s41556-026-01885-0
27. Wei G, Sun H, Dong K et al. The thermogenic activity of adjacent adipocytes fuels the progression of ccRCC and compromises anti-tumor therapeutic efficacy. Cell Metab. 2021; 33(10):2021-39 e8. https://doi.org/10.1016/j.cmet.2021.08.012
28. Clement E, Lazar I, Attane C et al. Adipocyte extracellular vesicles carry enzymes and fatty acids that stimulate mitochondrial metabolism and remodeling in tumor cells. EMBO J. 2020; 39(3):e102525. https://doi.org/10.15252/embj.2019102525
29. Tabe Y, Yamamoto S, Saitoh K et al. Bone Marrow Adipocytes Facilitate Fatty Acid Oxidation Activating AMPK and a Transcriptional Network Supporting Survival of Acute

Monocytic Leukemia Cells. Cancer Res. 2017; 77(6):1453-64. https://doi.org/10.1158/0008-5472.CAN-16-1645
30. Mukherjee A, Chiang CY, Daifotis HA et al. Adipocyte-Induced FABP4 Expression in Ovarian Cancer Cells Promotes Metastasis and Mediates Carboplatin Resistance. Cancer Res. 2020; 80(8):1748-61. https://doi.org/10.1158/0008-5472.CAN-19-1999
31. Yin JY, Zhang JT, Zhang W et al. eIF3a: A new anticancer drug target in the eIF family. Cancer Lett. 2018; 412:81-7. https://doi.org/10.1016/j.canlet.2017.09.055
32. Jiang SL, Wang ZB, Zhu T et al. The Downregulation of eIF3a Contributes to Vemurafenib Resistance in Melanoma by Activating ERK via PPP2R1B. Front Pharmacol. 2021; 12:720619. https://doi.org/10.3389/fphar.2021.720619
33. Zhang Y, Yu JJ, Tian Y et al. eIF3a improve cisplatin sensitivity in ovarian cancer by regulating XPC and p27Kip1 translation. Oncotarget. 2015; 6(28):25441-51. https://doi.org/10.18632/oncotarget.4555
34. Zheng X, Wang S, Hong S et al. Knockdown of eIF3a attenuated cell growth in K1 human thyroid cancer cells. Genes Genomics. 2021; 43(4):379-88. https://doi.org/10.1007/s13258-021-01048-5
35. Huo C, Wu D, Li X et al. eIf3a mediates malignant biological behaviors in colorectal cancer through the PI3K/AKT signaling pathway. Cancer Biol Ther. 2024; 25(1):2355703. https://doi.org/10.1080/15384047.2024.2355703
36. Lieber MR. The mechanism of double-strand DNA break repair by the nonhomologous DNA end-joining pathway. Annu Rev Biochem. 2010; 79:181-211. https://doi.org/10.1146/annurev.biochem.052308.093131

Figure and table legends

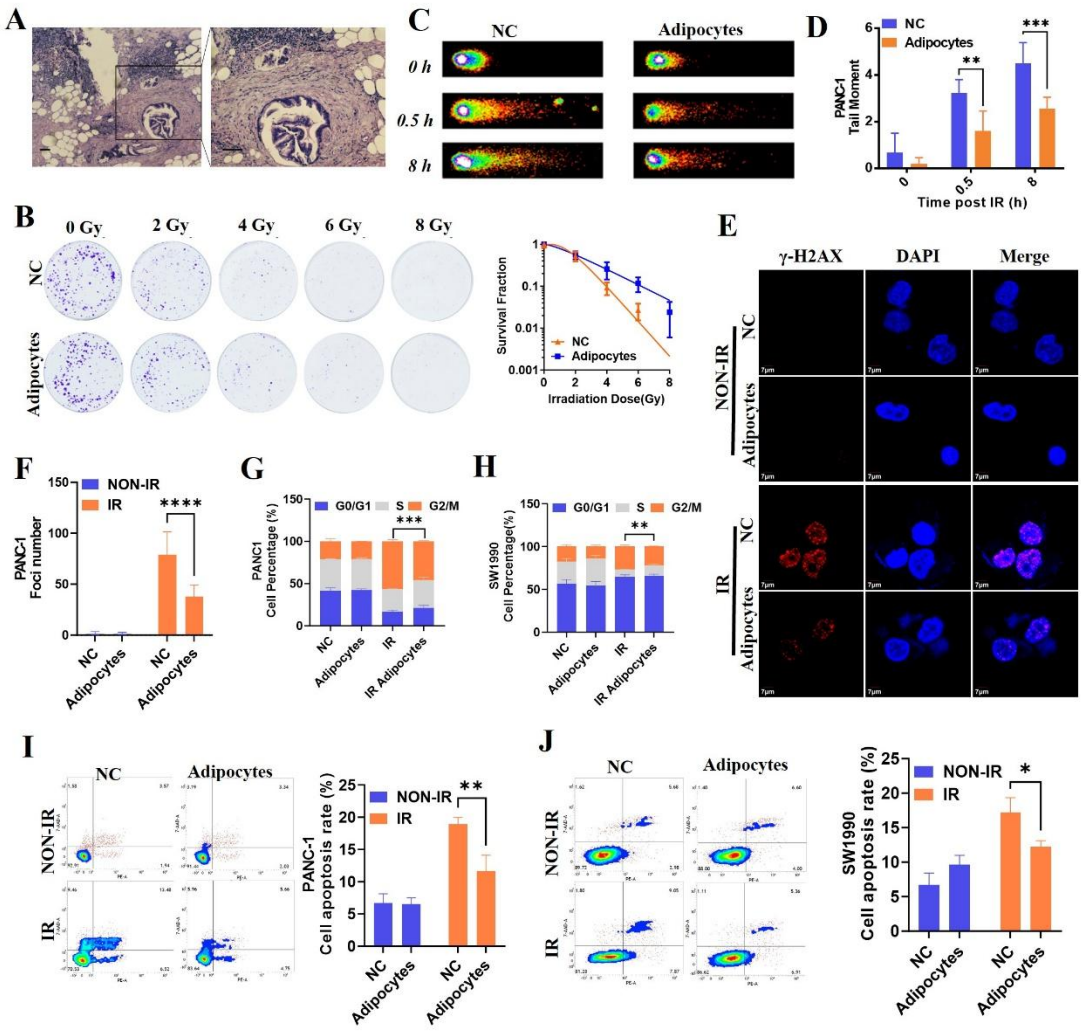


Figure 1. Adipocytes promote radioresistance of pancreatic cancer cells.

(A) Representative H&E staining images of tissue sections from pancreatic cancer patients. (B–J) PANC-1 or SW1990 cells were co-cultured with or without adipocytes and then exposed to radiation, unless otherwise indicated. (B) Colony formation assay of PANC-1 cells co-cultured with or without adipocytes. Colony numbers were quantified from three independent experiments and statistically analyzed. (C) Alkaline comet assay showing single-strand breaks (SSBs) in the DNA of PANC-1 cells. (D) Quantification of comet tail lengths; data are presented as mean ± standard deviation

(SD). (E) Immunofluorescence detection of γ-H2AX-positive foci. (F) Number of γ-H2AX-positive foci per nucleus counted using ImageJ software; results are mean ± SD. (G–J) PANC-1 and SW1990 cells co-cultured with adipocytes were irradiated and, after 24 hours, subjected to flow cytometry. Three independent experiments were performed. (G, H) Cell cycle distribution analysis. (I, J) Apoptosis analysis of pancreatic cancer cells. Statistical data from three independent experiments are presented.

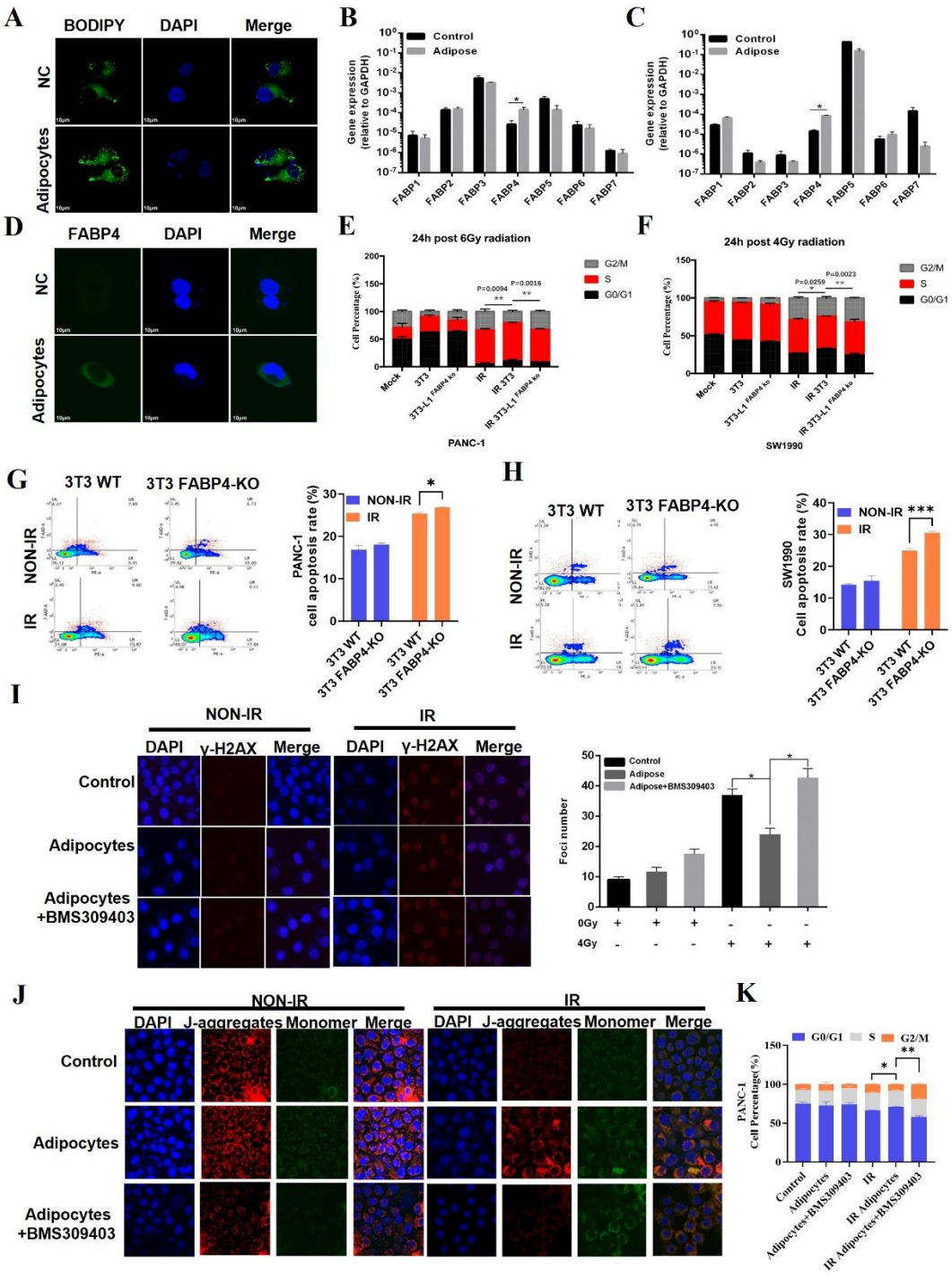


Figure2. FABP4 mediates adipocyte-triggered radioresistance in pancreatic cancer cells.

(A) Representative confocal microscopy images of lipid droplets in PANC-1 cells stained with BODIPY 493/503. (B, C) The expression of FABPs family mRNAs in human pancreatic cancer cells co-cultured with human adipose tissue was examined by

quantitative real-time PCR. PANC-1 cells are shown in (B) and SW1990 cells in (C). Data are presented as mean ± SD from three independent experiments. (D) Representative images of FABP4 staining in PANC-1 cells. (E, F) PANC-1 (E) and SW1990 (F) cells were co-cultured with 3T3-L1 adipocytes with or without FABP4 knockdown, followed by radiation exposure. Cell cycle distribution was analyzed by flow cytometry. Three independent experiments were performed, and the statistical data are presented. (G, H) Apoptosis of pancreatic cancer cells was assessed by flow cytometry under the same experimental conditions. Three independent experiments were conducted, and the resulting statistical data are shown. (I–K) The effects of FABP4 inhibitor treatment on pancreatic cancer cells co-cultured with adipocytes were examined. γ-H2AX foci formation (I), Mitochondrial membrane potential (J), and cell cycle distribution (K) were analyzed. Three independent experiments were performed, and the statistical data are presented.

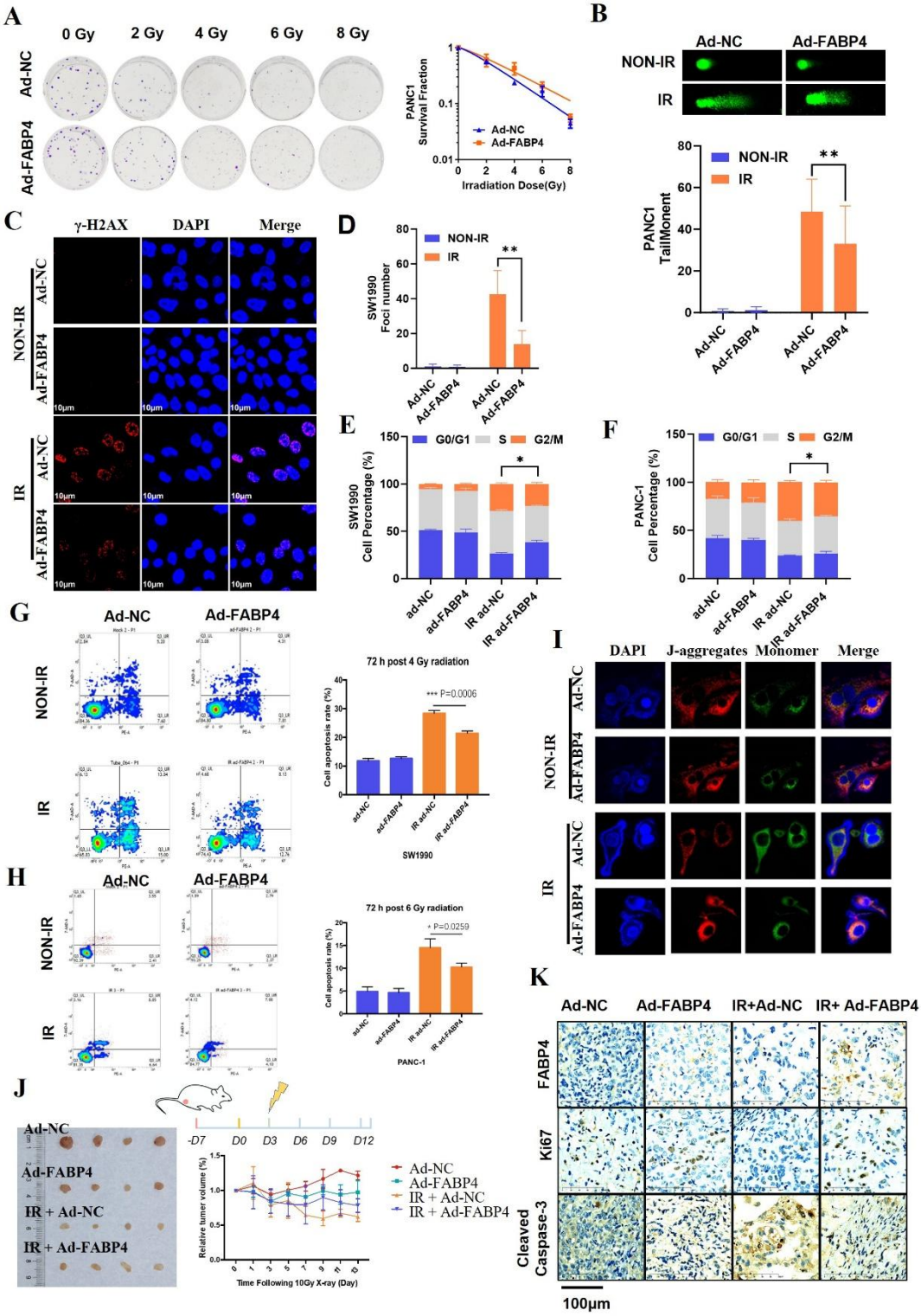
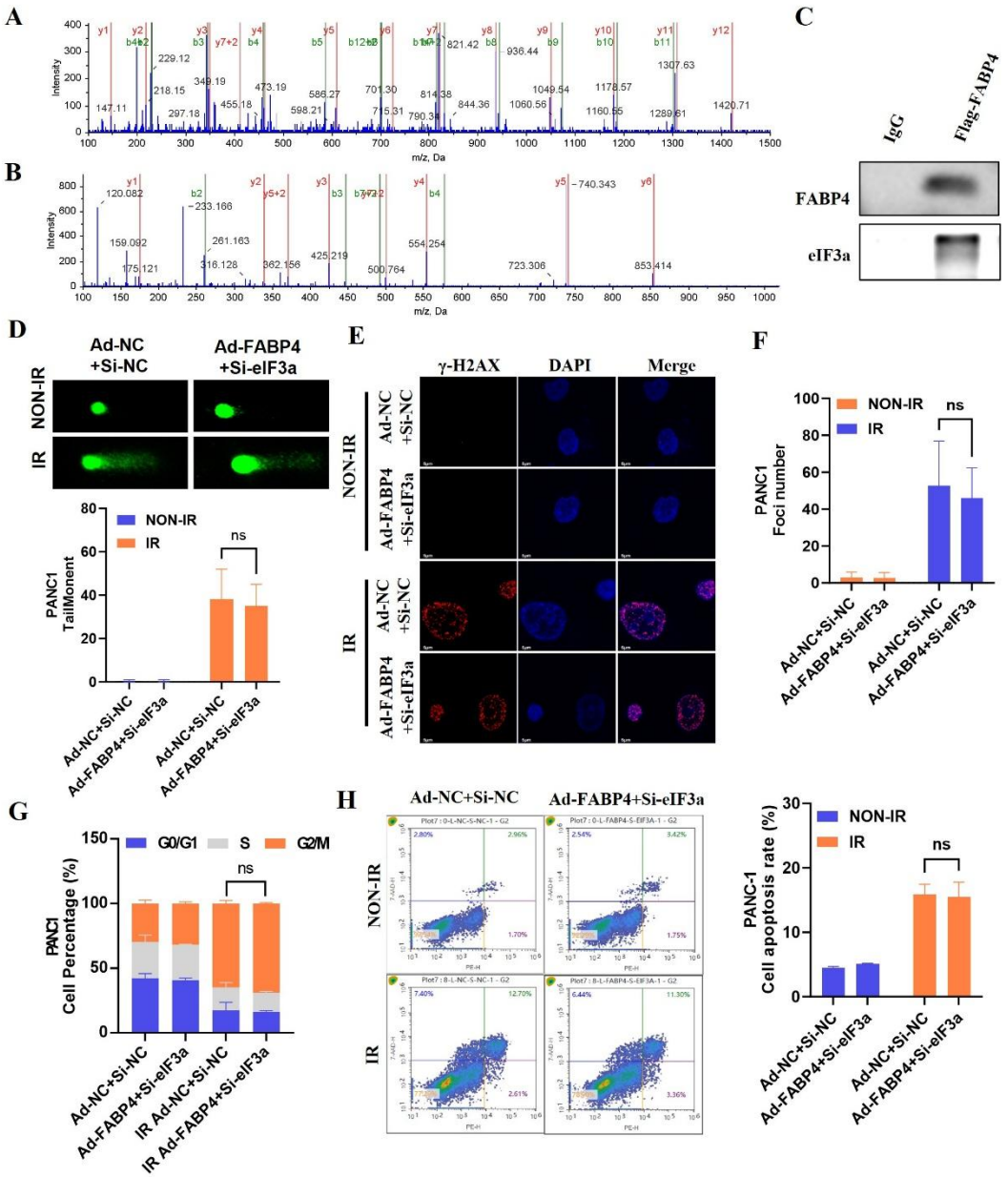


Figure 3. FABP4 regulates the radiosensitivity of pancreatic cancer both in vitro and in vivo.

(A) Clonogenic survival assay of PANC-1 cells overexpressing endogenous FABP4

(ad-FABP4) or negative control (ad-NC). Cells were exposed to increasing doses of radiation, and surviving fractions were calculated. Data are shown as mean ± SD from three independent experiments. (B) Alkaline comet assay showing single-strand breaks (SSBs) in the DNA of PANC-1 cells. Quantification of comet tail lengths; data are presented as mean ± standard deviation (SD). (C) Representative immunofluorescence images of γ-H2AX foci in irradiated SW1990 cells with or without FABP4 overexpression. (D) Quantification of foci per nucleus is shown. Three independent experiments were performed. (E–H) Flow cytometry analysis of cell cycle (E, F) and apoptosis (G, H) in PANC-1 and SW1990 cells following endogenous FABP4 upregulation and irradiation. Three independent experiments were performed, and the statistical results are shown. (I) The mitochondrial membrane potential was subsequently evaluated using a JC-1 fluorescent probe. All data are presented as mean ± SD from at least three independent biological replicates. (J) In vivo tumor growth assay. Nude mice bearing subcutaneous PANC-1 tumors (Ad-NC or Ad-FABP4) were exposed to IR (6 Gy). Tumor volumes were measured at indicated time points (n = 4 mice per group). (K) Immunohistochemical analysis of FABP4, Ki67, and cleaved caspase-3 expression changes in subcutaneous xenograft tumors of nude mice.



628

629 **Figure 4. eIF3a mediates FABP4-induced radioresistance in pancreatic cancer**

630 **cells.**

631 (A, B) LC-MS/MS tandem mass spectrum for the peptide sequence similar to eIF3a.

632 (A) A detail of the 1061.0 Da peptide MS/MS spectrum, matched to the sequence

633 DIDIEDLEELDPDFIMAK of eIF3a. (B) A detail of the 500.7 Da peptide MS/MS

634 spectrum, matched to the sequence FLWESYR of eIF3a. (C) FABP4 interacts with

635 eIF3a in human pancreatic cancer PANC-1 cells. (D) Alkaline comet assay showing

single-strand breaks (SSBs) in the DNA of PANC-1 cells. Quantification of comet tail lengths; data are presented as mean ± standard deviation (SD). (E, F) γ-H2AX foci formation in irradiated PANC-1 cells was examined by immunofluorescence staining. (G) Flow cytometry analysis of cell cycle in PANC-1 following Ad-FABP4 and irradiation. Three independent experiments were performed, and the statistical results are shown. (H) Apoptosis of pancreatic cancer cells was analyzed by flow cytometry, and the corresponding statistical results are presented.

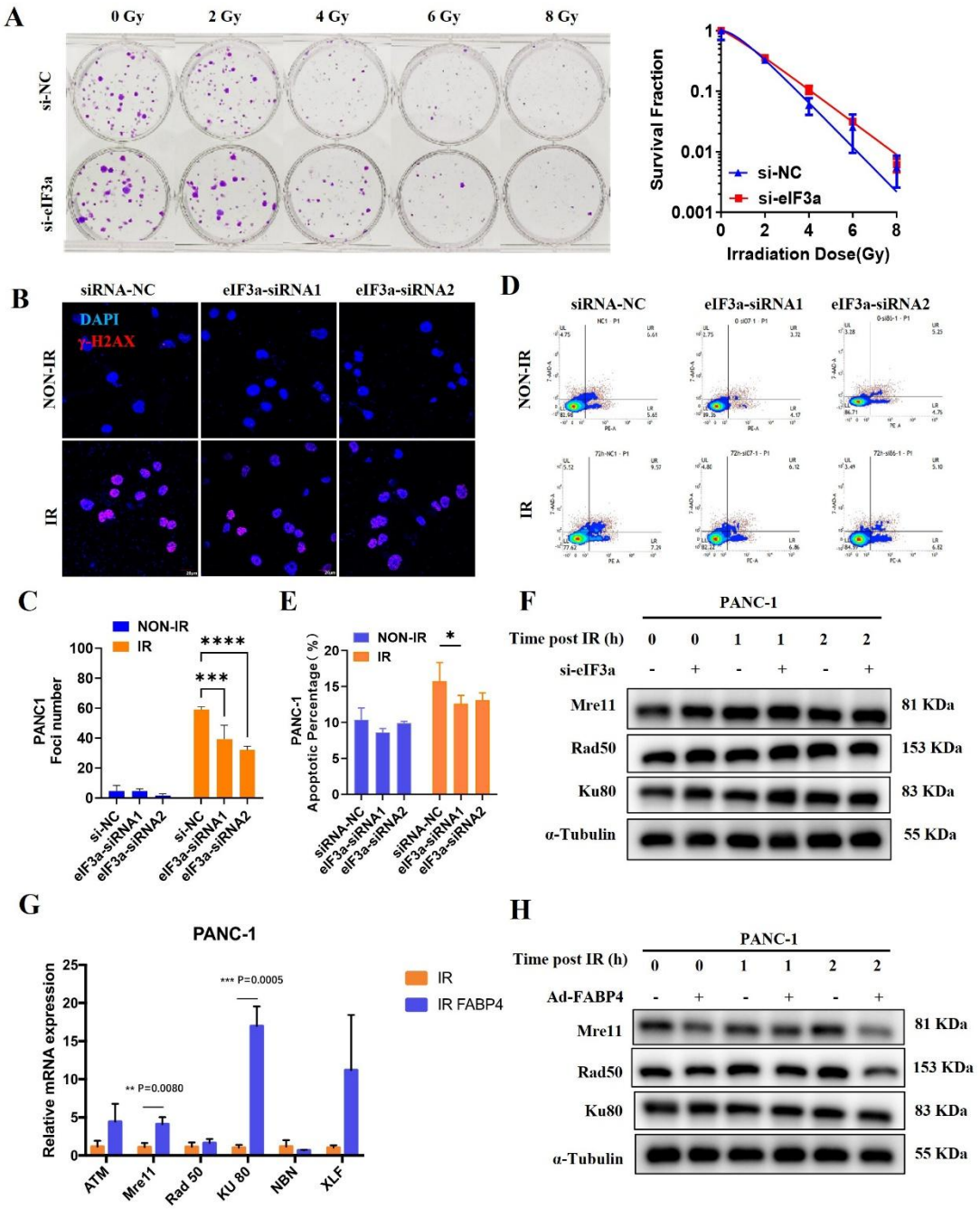


Figure 5. eIF3a mediates FABP4-induced radioresistance in pancreatic cancer cells independently of NHEJ signaling

(A) Colony formation assays showed that the proliferation of siRNA-eIF3a-transfected PANC-1 cells was suppressed by radiotherapy in a dose-dependent manner. (B, C) γ-H2AX foci formation in irradiated PANC-1 cells was examined by immunofluorescence staining. (D) Apoptosis of pancreatic cancer cells was analyzed

by flow cytometry, and the corresponding statistical results are presented. (E) KU80, RAD50, and MRE11 protein levels in PANC-1 cells after eIF3a knockdown. (F) Increased binding of eIF3a protein to *MRE11 and KU80* mRNA was observed in the FABP4-overexpressing group following IR. (G) KU80, RAD50, and MRE11 protein levels in PANC-1 cells after FABP4 overexpression.

Table 1 Top 30 proteins identified as FABP4-binding partners by LC-MS/MS

No.	Gene Names	Description	Category	Peptides (95%)
1	EIF3A	Eukaryotic Translation Initiation Factor 3 Subunit A	Protein Coding	55
2	EIF3B	Eukaryotic Translation Initiation Factor 3 Subunit B	Protein Coding	43
3	GAPVD1	GTPase Activating Protein And VPS9 Domains 1	Protein Coding	28
8	Krt2	Keratin 2	Protein Coding	20
4	EIF3C	Eukaryotic Translation Initiation Factor 3 Subunit C	Protein Coding	18
6	EIF3I	Eukaryotic Translation Initiation Factor 3 Subunit I	Protein Coding	14
7	ABCD3	ATP Binding Cassette Subfamily D Member 3	Protein Coding	14
5	EIF3G	Eukaryotic Translation Initiation Factor 3 Subunit G	Protein Coding	12
9	EIF3E	Eukaryotic Translation Initiation Factor 3 Subunit E	Protein Coding	7
10	VIM	Vimentin	Protein Coding	7
18	HBD	Hemoglobin Subunit Delta	Protein Coding	7
11	HSPA1A	Heat Shock Protein Family A (Hsp70) Member 1A	Protein Coding	7
14	IGHG3	Immunoglobulin Heavy Constant Gamma 3 (G3m Marker)	Protein Coding	6
12	EIF3L	Eukaryotic Translation Initiation Factor 3 Subunit L	Protein Coding	4
13	EIF4A1	Eukaryotic Translation Initiation Factor 4A1	Protein Coding	4
15	RPS3	Ribosomal Protein S3	Protein Coding	4
19	RPL13a	Ribosomal Protein L13a	Protein Coding	4
16	EIF3D	Eukaryotic Translation Initiation Factor 3 Subunit D	Protein Coding	3
17	HSPB1	Heat Shock Protein Family B (Small) Member 1	Protein Coding	3
20	RPL13AP3	Ribosomal Protein L13a Pseudogene 3	Pseudogene	4
21	SCAI	Suppressor Of Cancer Cell Invasion	Protein Coding	3
22	EEF1G	Eukaryotic Translation Elongation Factor 1 Gamma	Protein Coding	3
23	RAN	RAN, Member RAS Oncogene Family	Protein Coding	2
24	SLC25A5	Solute Carrier Family 25 Member 5	Protein Coding	2

25	RPS25	Ribosomal Protein S25	Protein Coding	2
26	EIF3M	Eukaryotic Translation Initiation Factor 3 Subunit M	Protein Coding	2
27	ALDOA	Aldolase, Fructose-Bisphosphate A	Protein Coding	2
28	RBMXL3	RBMX Like 3	Protein Coding	1
29	RBMXL2	RBMX Like 2	Protein Coding	1
30	ATP5B	ATP Synthase F1 Subunit Beta	Protein Coding	1

657

Supplementary Files

This is a list of supplementary files associated with this preprint. Click to download.

- Supplementarymethodsfiguresandtables.docx